SCIENTIFIC REPORTS

Hydatid detection using the near-infrared transmission angular spectra of porous silicon microcavity biosensors

Peng Li[1], Zhenhong Jia[2] & Guodong Lü[3]

Hydatid, which is a parasitic disease, occurs today in many regions worldwide. Because it can present a serious threat to people's health, finding a fast, convenient, and economical means of detection is important. This paper proposes a label- and spectrophotometer-free apparatus that uses optical biological detection based on porous silicon microcavities. In this approach, the refractive index change induced by the biological reactions of a sample in a porous silicon microcavity is detected by measuring the change in the incidence angle corresponding to the maximum transmitted intensity of a near-infrared probe laser. This paper reports that the proposed method can achieve the label-free detection of 43 kDa molecular weight hydatid disease antigens with high sensitivity.

Hydatid disease is a serious parasitic disease caused by the larvae of *Echinococcus granulosus* and *Echinococcus multilocularis* which affect both humans and animals[1–3]. The disease is most common in regions where animal husbandry is widespread. Parts of China, for instance, have some of the world's highest incidences of hydatid disease. Cystic hydatid disease is distributed mainly over China's northwest pastoral and farming regions. The infection rates of hydatid disease in a surveyed population reached 2.7% in Xinjiang[4], where the number of infected cases of hydatid disease each year is 54 times the national average. In such areas, convenient and low-cost detection methods are particularly important for achieving early diagnosis. Currently, the most common methods of detection involve imaging with B-mode ultrasound or computerized tomography and immunological testing with indirect haemagglutination assays and enzyme-linked immunosorbent assay kits. Obtaining high-definition images of hydatid cysts requires sophisticated and expensive equipment. Because doctors who use this method need both access to high-definition images and extensive experience in reading and interpreting the images, the method is not feasible in remote and less-developed areas. The immunological detection method offers low costs; however, the results obtained when testing the same antibody samples can vary with different detection kits. Furthermore, the detection sensitivity is low, which makes it difficult to screen out patients with weak immune responses. Thus, it is particularly important to look for a high-sensitivity, low-cost, and convenient immunological detection method for hydatid disease.

Porous silicon is a favourable material because of its large specific surface area, good biological activity, and adsorption properties[5,6]. It can also be produced easily in a variety of photonic devices. Biosensors based on porous silicon are used in biomedical diagnostics, environmental monitoring, and veterinary and food-quality control[7–15]. Among porous silicon biosensors with different optical structures, the porous silicon microcavity (PSM) offers very high sensitivity[16,17]. The most commonly used method for the detection of biological materials using porous silicon sensors is the reflection spectrum method that using a spectrophotometer, detecting the resonance peak shift of the wavelength corresponding to the resonance peak of the reflection spectrum before and after the biological reaction in the PSM. This approach is based on the reaction of biomolecules in the PSM causing the refractive index of the device to increase, resulting in a redshift of the reflection spectrum. This method has also been applied to the detection of protein kinase P38 for diagnosing hydatidosis hydatid disease[18].

However, for high sensitivity detection, a high resolution spectrophotometer is needed. For example, to measure a refractive index change of 10^{-4}, the resolution of the spectrophotometer must reach 0.01 nm[19]. It is difficult

[1]School of Physical Science and Technology, Xinjiang University, Urumqi 830046, China. [2]College of Information Science and Engineering, Xinjiang University, Urumqi 830046, China. [3]The First Affiliated Hospital of Xinjiang Medical University, Urumqi 830054, China. Correspondence and requests for materials should be addressed to Z.H.J. (email: jzhh@xju.edu.cn)
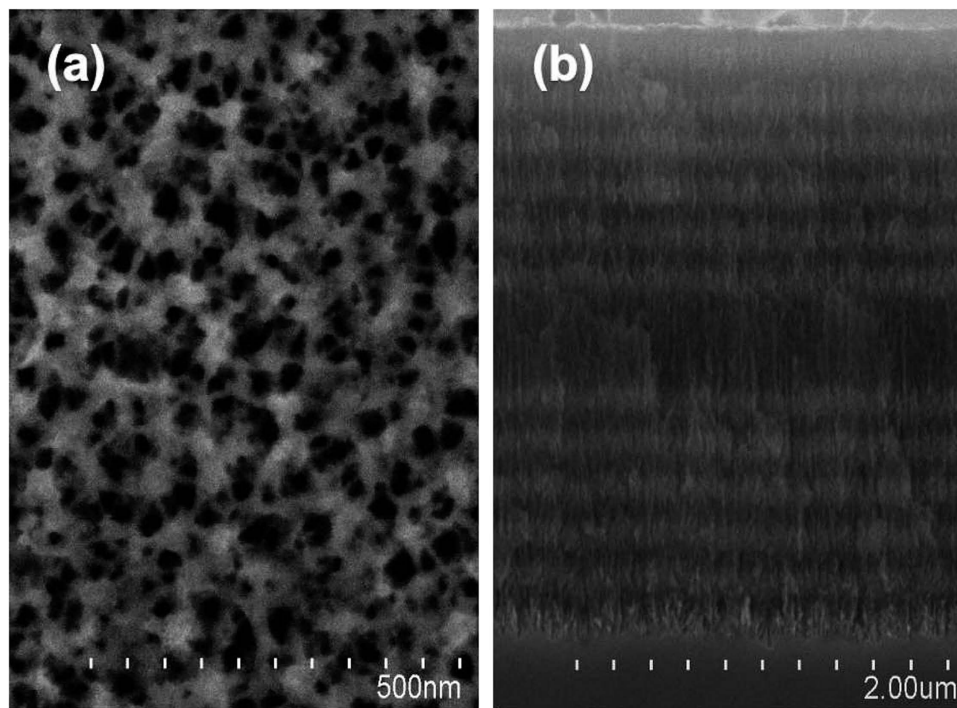
Figure 1. SEM image of (**a**) the top view of the surface (**b**) cross section of the PSM.

to apply this method in an ordinary laboratory because of the expense and bulk of the spectrophotometer. To solve this problem, Li *et al.* proposed a spectrophotometer-free detection method based on the reflection angular spectrum to achieve highly sensitive detection for eight base pairs of DNA[19]. A refractive index change of 10^{-4} in PSM can be detected by the reflection angular spectrum method. The detection system includes only one He-Ne laser, one detector and one ordinary goniometer (with a resolution of 1′). However, there are still some problems to be solved in this method: porous silicon shows strong absorption to visible light, which has a great influence on the optical properties of PSM. Furthermore, the visible wavelength laser beam may be harmful to some biological samples.

In this paper, we propose a new optical biosensor label-free detection method, which has successfully achieved the immune detection of hydatid disease. The refractive index change induced by biological reactions in PSM is measured based on the transmission angular spectrum of near-infrared laser light. Because the absorption of the near-infrared laser in porous silicon is very small, the desirable optical characteristics of PSM devices are exhibited, and the detection sensitivity increases. As near-infrared light is located in the optically transparent window of the biological sample, no damage to the biological samples results[20]. The transmission angular spectrum method is easier than the reflection angular spectrum method. In the reflection angular spectrum method, to prevent the detector form blocking the incident light, there must be a certain distance between the sample and the detector. The orientation and position of the detector must be continuously adjusted to ensure that all of the reflected light can be received, which is inconvenient for sensor detection. In the transmission angular spectrum method, the sensor is fixed at the centre of the rotary stage of the goniometer, and the detector is stationary, so the transmitted light angle of the sensor can be measured easily by rotating the stage. In our work, 43 kDa cystic hydatid disease antigens have been detected by the near-infrared transmitted angular spectrum method based on PSM, where detection limit was 0.16 ng/ml.

Material and Methods

Preparation of PSMs and functionalization. PSMs were prepared by electrochemical anodization of highly doped p-type silicon (boron doped, 0.03–0.06 Ω·cm resistivity) in a mixed solution, 1:1 by volume, composed of 40% aqueous hydrofluoric acid (Tianjin Zhiyuan Chemical Reagent Co., Ltd., Tianjin, China) and 99% alcohol (Tianjin Fuyu Fine Chemical Co., Ltd., Tianjin, China).

Silicon wafers (Tianjin Semiconductor Technology Research Institute, Tianjin, China) were cleaned with acetone (Tianjin Zhiyuan Chemical Reagent Co., Ltd., Tianjin, China), ethanol (Tianjin Zhiyuan Chemical Reagent Co., Ltd, Tianjin, China), and deionized (DI) water before use in the experiment. The silicon wafers were then anodized using the Labview program, which offered computerized control of the alternating current density and corrosion time. The current densities were 110 mA/cm² and 60 mA/cm²; corrosion times were 2.5 s and 3.0 s. For the microcavity, the current density and corrosion time were 110 mA/cm² and 5.0 s, respectively. Supplements increasing fluoride concentration and 3.0 s pauses were introduced after the formation of each layer to ensure that the corrosion was relatively uniform. Surface characterization data can be provided by SEM. Figure 1 shows that the diameter of the pores varies from 30 to 50 nm, and that the thickness of the PSM is approximately 3.5 μm.
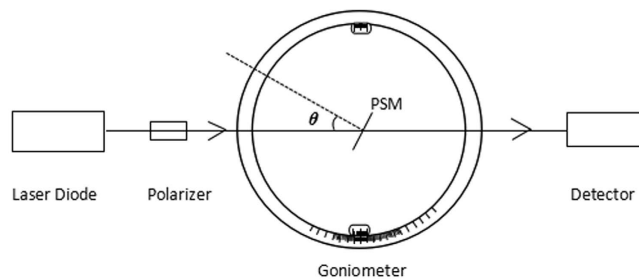
Figure 2. Experimental apparatus.

After preparing the PSMs, the functional processing was necessary. The PSMs were put into a 40% hydrogen peroxide (Tianjin Zhiyuan Chemical Reagent Co., Ltd.) solution at 60 °C and placed in a vacuum drying oven (DZF-6050, Shanghai Yiheng Scientific Instrument Co., Ltd., Shanghai, China) for 3 h. Then, the PSMs were removed and repeatedly rinsed with DI water before being allowed to air dry. Next, the PSMs were soaked for 1 h in a 5% aminopropyltriethoxysilane solution (10:10:1 = DI water:methanol:APTES (99%, Sigma-Aldrich, St. Louis, MO, USA)), flushed repeatedly with DI water, and then baked at 100 °C for 10 min in a vacuum drying oven. Finally, the PSMs were put into a 2.5% solution of glutaraldehyde (19:1 = DI water:GA (50%, Aladdin Reagent Co., Ltd., Shanghai, China)) for 1 h at room temperature 22 °C and washed three times with phosphate buffer solution (PBS, Shanghai Sangon Biotech Co., Ltd., Shanghai, China) to remove excess glutaraldehyde. The PSMs were then washed again with DI water.

Preparation of the biological probe and detection. After functionalization, hydatid antibody was selected as the probe. The PSMs were dropped into 20 μL of hydatid antibody (1:1000, obtained from rabbit serum, Xinjiang Key Laboratory of Hydatid Disease, Xinjiang, China) and then incubated for 2 h in a thermostat (Shanghai Jinghong Laboratory Instrument Co., Ltd., Shanghai, China), followed by cleaning with PBS and DI water. Finally, the PSMs were dipped into a concentration of 4% bovine serum albumin (BSA, Xinjiang Key Laboratory of Hydatid Disease, Xinjiang, China) for 1 h at 37 °C in the thermostat. The PSMs were then flushed with PBS and DI water and dried in air. The PSMs were placed on a goniometer stage with a measuring incidence angle θ_1 corresponding to the maximum transmitted intensity of a near-infrared probe laser.

The PSMs were dropped separately into 20 μL of a solution containing different concentrations of hydatid antigen (Xinjiang Key Laboratory of Hydatid Disease, Xinjiang, China) and incubated in the thermostat for 1 h. Then, all samples were rinsed repeatedly with PBS and DI water and allowed to air dry. The PSMs were again placed on the goniometer stage with a measuring incidence angle θ_2 corresponding to the maximum transmitted intensity of a near-infrared probe laser. The change in refractive index Δn can be determined from the change of the laser incident angle: $\Delta \theta = \theta_2 - \theta_1$.

Detection apparatus. Figure 2 shows the experimental device used to implement the proposed optical transmission biological detection method based on the PSM. The device included a laser diode (Changchun New Industries Optoelectronics Tech Co., Ltd., Changchun, China), polarizer (Changchun No.1 Optical Instrument Factory, Changchun, China), goniometer (Changchun No.1 Optical Instrument Factory, Changchun, China), and detector (Thorlabs Inc., Newton, NJ, USA). The laser was a high-stability and power-tunable near-infrared semiconductor laser with a divergence angle of 1 mrad and a wavelength of 1550 nm.

Theory and method. When the laser was incident on the PSM at different angles, the position of the transmission spectrum changed. In the experiment, the incident light was a transverse electric wave, and the refractive indices of the PS dielectric-layer were 1.21 and 1.52. The microcavity refractive index layer was also designed to exhibit a refractive index of 1.21. The optical thickness nd (where n is the refractive index, and d is the physical thickness) was set to two times nd of the dielectric layer PS. On both sides of the Bragg layer, the number of cycles was six. The reference wavelength λ_C was 1550 nm. The PSM device was designed to match these parameters. The incident light angle θ was adjusted to 0°, 10°, 20°, and 30° for theoretical simulation by Bruggeman effective medium approximation[21] and the transfer matrix method[22,23]. The calculation results indicated that the transmission peaks were located at 1550 nm, 1536 nm, 1497 nm, and 1434 nm, respectively. Figure 3(a) shows the PSM transmission spectra, which demonstrate that when the incident angle increased, the transmission spectrum of the PSM underwent a blueshift.

In the incident beam with normal incidence ($\theta = 0°$) and a corresponding transmission peak wavelength λ_C of 1550 nm, the refractive index of each dielectric layer of the porous silicon increased ($\Delta n = 0.01$) when a biological response occurred in the PSM device. Thus, the transmission spectrum experienced a redshift, and the transmission peak wavelength of the transmitted light underwent a corresponding increase $\Delta \lambda_C$ of 11.7 nm. These results, labelled as cases 1 and 2, appear in Fig. 3(b). When the incident angle of the light source increased to 9.37°, the transmission peak λ_C of the PSM remained unchanged from the condition of vertical incidence, indicating that these two transmission peaks overlapped, as shown in Fig. 3(b) by cases 3 and 1, respectively. Figure 3(b) also shows that for the PSM device, when $\Delta n = 0.01$, $\Delta \lambda_C = 11.7$ nm. This approsch is the common method to obtain the refractive index change from the transmission spectrum. However, another new method is proposed for measuring the refractive index change of PSM devices. A single-wavelength infrared laser, with wavelength λ_i
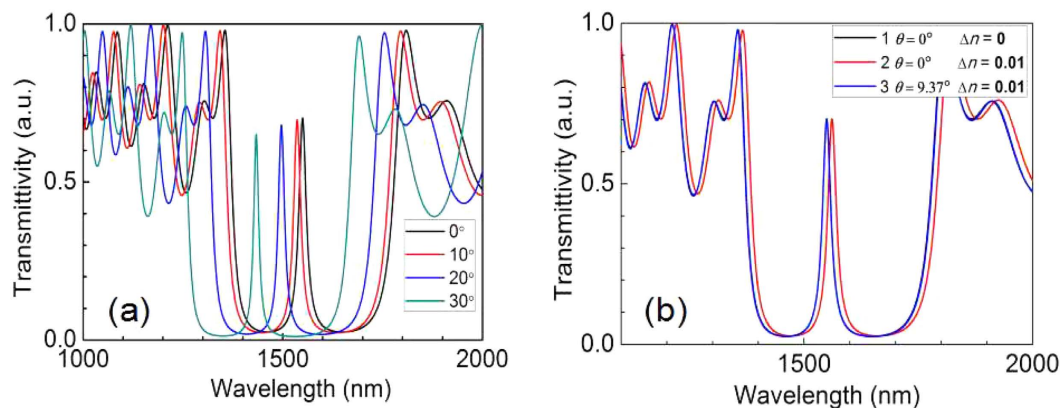
Figure 3. Transmission spectra for various angles. (**a**) PSM transmission spectra of for various incident angles ($\theta = 0°$). (**b**) Curve 1 represents the PSM transmission spectrum of vertical incidence ($\theta = 0°$); curve 2 represents the occurrence in the PSM device of a biological reaction that caused the refractive index to increase to $\Delta n = 0.01$, identical to a PSM transmission spectrum with vertical incidence ($\theta = 0°$); curve 3 represents the PSM transmission spectrum after a certain rotary angle of incident light.

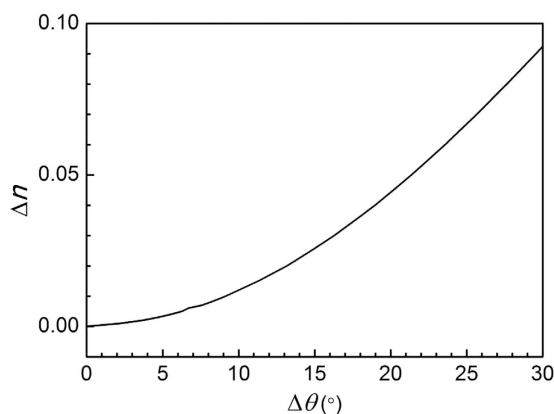**Figure 4. Relationship between $\Delta \theta$ and Δn.**

equal to the designed λ_C, is used to irradiate the PSM device at normal incidence without reflection. When the PSM device with a laser vertically incident shows changes in its refractive index because of the biological reaction, the transmitted light will be weakened. If the incident laser beam is adjusted to a certain angle of θ, all of the light will be transmitted. Thus, the refractive index change Δn caused by the change in the incident angle of the laser $\Delta \theta$ can be obtained. Figure 4 shows, in theoretical calculations, the relationship between the refractive index Δn and $\Delta \theta$.

The PSM refractive index increases by Δn because of the antigen-antibody reaction. When the change in refractive index Δn increases to 10^{-4}, we can use the transfer matrix method to calculate that $\Delta \theta = 0.046°$ and $\Delta \lambda_C = 0.05$ nm. The resolution of the general angle measuring instrument is 1, that is, 0.0167°. It can detect a change of value Δn of 10^{-4}. The resolution of the optical experiment equipment for laboratory spectral detection (U-4100 UV-Vis-NIR Double Beam Spectrophotometer, Hitachi High-Technologies Corporation, Tokyo, Japan) is 0.1 nm; thus, it cannot detect a Δn of 10^{-4}. An expensive spectrophotometer with a resolution of 0.01 nm would be required to detect such an increase in Δn.

Figure 5 shows both the change in incident angle and the microcavity on both sides of the Bragg layers over six cycles of laser transmittivity. The black lines in the graph show the transmitted angular spectra, indicating that the refractive index of the porous silicon microcavity device remains unchanged. The red lines indicate the transmitted angular spectra of the porous silicon microcavity device after the refractive index changed, where $\Delta n = 0.001$. In cases where the laser beam was incident near an angle of 25°, a detectable amount of movement for the transmitted angular spectrum of PSM was more obvious.

Results and Discussion

After each step in the function of the PSM, the oblique incident angle was used to detect and confirm each step of the chemical connection. Figure 6(a) shows the changes in angle with the PSM function as each step occurred. They are as follows, from left to right: after oxidation, after silanization, and after the addition of glutaraldehyde. Figure 6(b) illustrates the detection of the hydatid antibody in the PSM. The transmitted angular spectrum
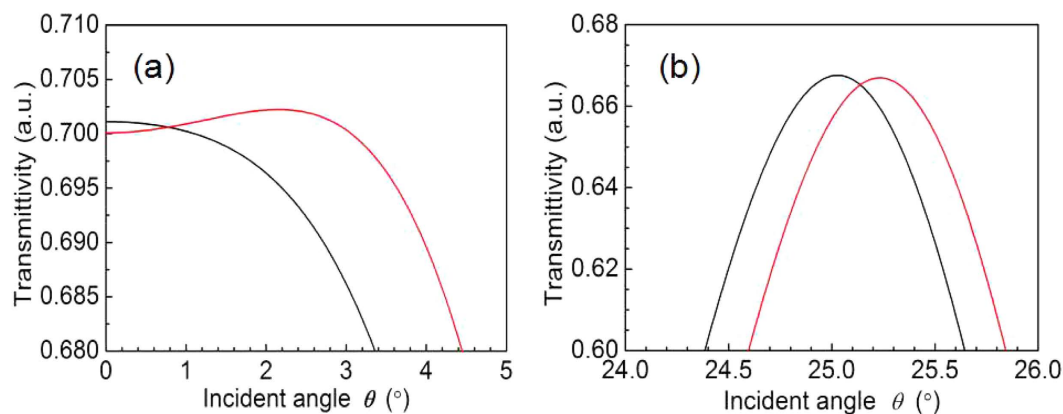
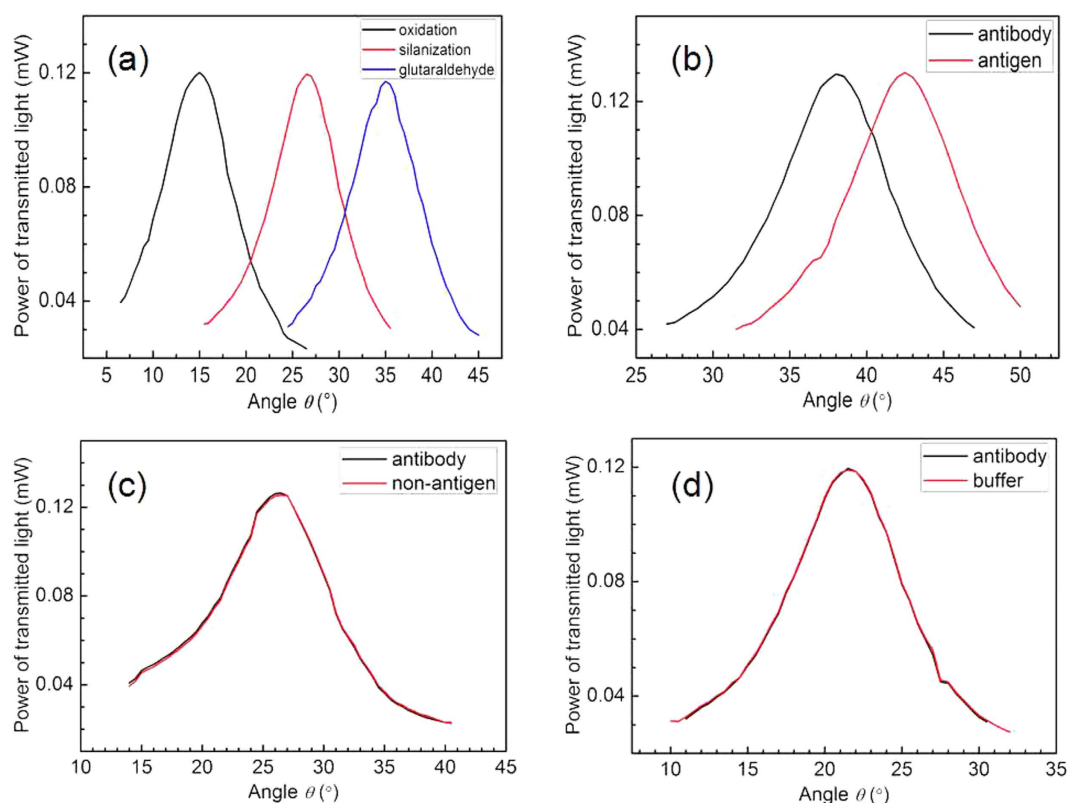**Figure 5.** Transmission angular spectra (**a**) near 0° and (**b**) near 25°.

Figure 6. Power of transmitted light under various conditions. (**a**) Transmission angular spectra corresponding to changes in the PSM functional steps: after oxidation, after silanization, and after the addition of glutaraldehyde. (**b**) The PSM transmission angular spectra changes for the hydatid antigen. (**c**) Negligible PSM transmission angular spectra changes for a non-hydatid antigen. (**d**) No change in the PSM transmission angular spectra reaction to the buffer solution.

shifted approximately 4.54° after the PSM in which the probe was immobilized was exposed to 2×10^{-6} mg/ml of hydatid antigen. The effective refractive index change was due primarily to the effective combination of the hydatid antigen and immobilized probe in the PSM device. To demonstrate specificity, Fig. 6 (c) and (d) show the transmitted angular spectra exhibiting a negligible shift after exposure to a non-hydatid antigen and to a buffer solution (which must be flushed with DI water), respectively. The negligible shifts in the angle spectra may arise from the fact that the probe and non-hydatid antigen do not combine in the PSM, thus yielding no change in the effective refractive indices.

Figure 7 shows the shift in the transmission angular spectra for the hydatid antigen at different concentrations: 0.5×10^{-6}, 1.0×10^{-6}, 2.0×10^{-6}, 1.0×10^{-5}, and 2.0×10^{-5} mg/ml (Table 1). These results indicate that the angle variations corresponding to these concentrations were 1.52°, 2.46°, 4.54°, 12.88°, and 26.36°, respectively. Figure 7 also demonstrates a strong linearity (R = 0.959) between the shift of the transmitted angular spectrum
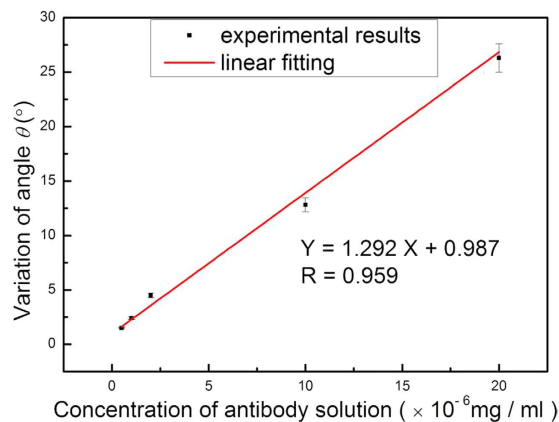
Figure 7. Linear relationship diagram for transmission angular spectrum changes with concentrations of hydatid antigen varying from 0.5×10^{-6} mg/ml to 2.0×10^{-5} mg/ml.
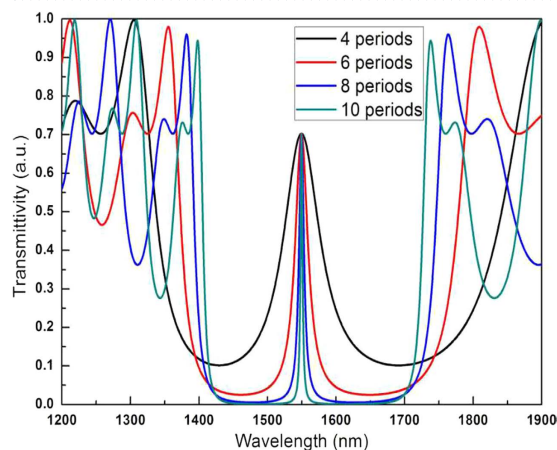

Figure 8. PSM transmission spectra of different periods.

	Transmittance angle θ (°)						$\overline{Y}$ (°)	S (°)	RSD (%)	$\overline{Y} \pm S$ (°)
	Y_1	Y_2	Y_3	Y_4	Y_5	Y_6				
Probe + antigen (0.5×10^{-6} mg/ml)	1.64	1.44	1.50	1.56	1.58	1.40	1.52	0.09	6.0	1.52 ± 0.09
Probe + antigen (1.0×10^{-6} mg/ml)	2.62	2.46	2.38	2.56	2.32	2.42	2.46	0.11	4.5	2.46 ± 0.11
Probe + antigen (2.0×10^{-6} mg/ml)	4.20	4.64	4.58	4.36	4.88	4.58	4.54	0.24	5.3	4.54 ± 0.24
Probe + antigen (1.0×10^{-5} mg/ml)	13.26	13.34	12.38	13.32	12.30	12.68	12.88	0.49	3.8	12.88 ± 0.49
Probe + antigen (2.0×10^{-5} mg/ml)	27.28	25.10	26.98	28.24	25.34	25.22	26.36	1.32	5.0	26.36 ± 1.32

Table 1. Experimental datas. The average value of the experiment as a result. Sensitivity and reproducibility of the PSM biosensor after exposure to different concentration of hydatid antigen in Fig. 7. $Y_1, Y_2, Y_3, Y_4, Y_5, Y_6$ are transmittance angle θ corresponding to these six samples, $\overline{Y}$ is average value of transmittance angle θ, S is standard deviations, and RSD is relative standard deviation, where $S = \sqrt{\frac{\sum_{i=1}^{n}(X_i - \overline{X})^2}{n-1}}$, $RSD = \frac{S}{\overline{X}} \times 100\%$.

and the concentration of hydatid antigen in the range from 0.5×10^{-6} mg/ml to 2×10^{-5} mg/ml. The equation of linear regression was determined to be $Y = 1.292\,X + 0.987$, where Y represents the shift of the transmitted angular spectrum and X the concentration of hydatid antigen. Taking into account the stability of the light detector in this experiment and the interface roughness of each layer in the PSM, the actual angle measurement resolution was approximately 0.2°. Therefore, the detection limit of the biosensor was 0.16 ng/ml. Several relevant bioassays based on porous silicon have been reported: a nanoscale porous silicon microcavity biosensor for novel label-free tuberculosis antigen-antibody detection with a limit of 5.4 μg/ml[24]; an antifreeze protein detection using Rhodamine B as a photoluminescence label in porous silicon with a limit of 16.5 ng/ml[25]; and a novel multilayered

porous silicon-based immunosensor for determining hydroxy-safflor yellow A with a limit of 0.78 ng/ml[26]. One study reports a porous silicon resonant microcavity biosensor for matrix metalloproteinase detection with a limit as low as $7.5 \times 10^{-19} M$[27] because this biosensor is based on fluorescence detection, the limit of detection is lower.

The full width at half maximum (FWHM) of the transmitted angle spectrum will change with differences in the Bragg layer cycles and will affect the amount of change in the refractive index arising from changes caused by transmittance. If too few cycles of the Bragg layers occur on both sides of the microcavity, then the lower number of cycles will result in deterioration of the photonic crystal device characteristics, an increase in the FWHM of the transmitted angular spectrum, and a decrease in detection sensitivity. An excessive number of cycles makes it difficult for biomolecules to integrate into each layer of the PSM device. In the bioassay of hydatid disease, experiments indicated that the detection result was optimized if the Bragg layer was six cycles. Figure 8 shows the PSM transmission spectra of different periods. The FWHM of the transmission spectra becomes narrower with increasing cycles.

This paper proposed biosensors based on the PSM optical transmission angular spectra detection method to achieve the detection of the 43 kDa hydatid disease antigen. At a biosensor sensitivity of 1.30°/ng/ml, the detection limit was 0.16 ng/ml. The transmission angular spectra measurement method was adopted in this experiment, mainly to avoid the absorption of porous silicon and to increase the detection sensitivity. Thus, no light damage occurred in the biological sample. More importantly, the detection process was easier. Therefore, this optical biosensor, based on PSM and using the near-infrared transmitted angular spectrum for the detection of cystic hydatid disease, can offer a fast, convenient, and economical means of detection; thus, it can be widely promoted and applied in remote pastoral areas.

References

1. McManus, D. P., Zhang, W., Li, J. & Bartley, P. B. Echinococcosis. *Lancet.* **362,** 1295–1304 (2003).
2. World Health Organization. Working to overcome the global impact of neglected tropical diseases: First WHO report on neglected tropical diseases. *WHO* (2010).
3. Restrepo, A. M. C. *et al.* The landscape epidemiology of echinococcoses. *Infect. Dis. Pov.* **5,** 1 (2016).
4. Nusilaiti, *et al.* Echinococcosis (hydatid disease) infection in livestock in 14 areas in Xinjiang, 2014. *Chin. J. Zoonoses.* **32(2),** 202–205 (2016).
5. Low, S. P., Williams, K. A., Canham, L. T. & Voelcker, N. H. Evaluation of mammalian cell adhesion on surface-modified porous silicon. *Biomaterials.* **27,** 4538–4546 (2006).
6. Tessier, D. C., Boughaba, S., Arbour, M., Roos, P. & Pan, G. Improved surface sensing of DNA on gas-etched porous silicon. *Sens. Actuators B: Chem.* **120,** 220–230 (2006).
7. Lin, V. S.-Y., Motesharei, K., Dancil, K. P. S., Sailor, M. J. & Ghadiri, M. R. A porous silicon-based optical interferometric biosensor. *Science.* **278,** 840–843 (1997).
8. Dancil, K. P. S., Greiner, D. P. & Sailor, M. J. A porous silicon optical biosensor: detection of reversible binding of IgG to a protein A-modified surface. *J. Am. Chem. Soc.* **121,** 7925–7930 (1999).
9. Mulloni, V. & Pavesi, L. Porous silicon microcavities as optical chemical sensors. *Appl. Phys. Lett.* **76,** 2523–2525 (2000).
10. Chan, S., Fauchet, P. M., Li, Y., Rothberg, L. J. & Miller, B. L. Porous silicon microcavities for biosensing applications. *Phys. Status Solidi A.* **182,** 541–546 (2000).
11. Chan, S., Li, Y., Rothberg, L. J., Miller, B. L. & Fauchet, P. M. Nanoscale silicon microcavities for biosensing. *Mater. Sci. Eng. C.* **15,** 277–282 (2001).
12. Alvarez, S. D. *et al.* Using a porous silicon photonic crystal for bacterial cell-based biosensing. *Phys. Status Solidi A.* **204,** 1439–1443 (2007).
13. Jane, A., Dronov, R., Hodges, A. & Voelcker, N. H. Porous silicon biosensors on the advance *Trends Biotechnol.* **27,** 230–239 (2009).
14. Giovannozzi, A. M. *et al.* P450-based porous silicon biosensor for arachidonic acid detection. *Biosens. Bioelectron.* **28,** 320–325 (2011).
15. Acquaroli, L. N., Kuchel, T. & Voelcker, N. H. Towards implantable porous silicon biosensors. *RSC Adv.* **4,** 34768–34773 (2014).
16. Zhang, H. Y. *et al.* Porous silicon optical microcavity biosensor on silicon-on-insulator wafer for sensitive DNA detection. *Biosens. Bioelectron.* **44,** 89–94 (2013).
17. Lv, X. Y. *et al.* Hybridization assay of insect antifreezing protein gene by novel multilayered porous silicon nucleic acid biosensor. *Biosens. Bioelectron.* **39,** 329–333 (2013).
18. Lv, X. Y., Lv, G. D., Jia, Z. H., Wang, J. J. & Mo, J. Q. Detection of protein kinases P38 based on reflectance spectroscopy with n-type porous silicon microcavities for diagnosing hydatidosis hydatid disease. *SPIE Proceedings,* **9268,** doi: 10.1117/12.2071332 (2014).
19. Li, P. *et al.* Spectrometer-free biological detection method using porous silicon microcavity devices. *Opt. Express.* **23,** 24626–24633 (2015).
20. Del Milagro Fernández-Carrobles, M., Bueno, G., Déniz, O., Salido, J. & García-Rojo, M. Automatic handling of tissue microarray cores in high-dimensional microscopy images. *IEEE J. Biomed. Health Inform.* **18,** 999–1007 (2014).
21. Bruggeman, D. A. G. Calculation of various physics constants in heterogenous substances I Dielectricity constants and conductivity of mixed bodies from isotropic substances. *Ann. Phys.* **416,** 636–664 (1935).
22. Born, M. & Wolf, E. *Principles of Optics.* (6th ed. Pergamon, Oxford, 1980).
23. Yeh, P. *Optical Waves in Layered Media.* (Wiley, New York, 1988).
24. Wu, B. *et al.* A nanoscale porous siliconmicrocavity biosensor for novel label-free tuberculosis antigen–antibody detection. *Nano.* **7,** 1250049 (2012).
25. Zhang, H. Y. *et al.* Antifreeze protein detection using Rhodamine B as photoluminescence label in porous silicon. *Curr. Appl. Phys.* **13,** 736–742 (2013).
26. Lv, X. Y. *et al.* Novel multilayered porous silicon-based immunosensor for determining Hydroxysafflor yellow A. *Appl. Surf. Sci.* **257,** 1906–1910 (2011).
27. Krismastuti, F. S. H., Pace, S. & Voelcker, N. H. Porous silicon resonant microcavity biosensor for matrix metalloproteinase detection. *Adv. Funct. Mat.* **24,** 3639–3650 (2014).

Acknowledgements

Author Contributions

Z.H.J. designed research. P.L. performed the experiments. P.L. and Z.H.J. wrote the manuscript. G.D.L. Provided biological samples. P.L. analyzed the data. All authors read and approved the final manuscript.

Additional Information

Competing Interests: The authors declare no competing financial interests.

How to cite this article: Li, P. *et al.* Hydatid detection using the near-infrared transmission angular spectra of porous silicon microcavity biosensors. *Sci. Rep.* **7**, 44798; doi: 10.1038/srep44798 (2017).

Publisher's note: Springer Nature remains neutral with regard to jurisdictional claims in published maps and institutional affiliations.